

Quasiclassical R -matrix theory of inelastic processes in collisions of electrons with HCl molecules

I. I. Fabrikant

Department of Physics and Astronomy, University of Nebraska, Lincoln, Nebraska 68588-0111

(Received 10 September 1990)

The R -matrix theory for the vibrational excitation and dissociative attachment in e -HCl collisions is developed. Only one pole in the R -matrix expansion is included. This allows for making a connection between the R -matrix and the nonlocal-complex-potential theories, and for obtaining the expression for the dissociative-attachment cross section without using the R -matrix radius in the internuclear coordinate. All matrix elements in the equation for the vibrational-excitation and dissociative-attachment amplitudes are calculated using the quasiclassical approach. We study how the results depend on the number of vibrational levels of the neutral molecule included in the theory and show how to exclude the vibrational continuum by a modification of the nonlocal-complex potential. The results for the vibrational-excitation cross sections are extremely sensitive to the behavior of the R -matrix potential curve near the point of crossing this curve with the potential curve of the neutral molecule. Particularly in some cases the cross section at the threshold peak exhibits the boomerang oscillations earlier found for HCl by Domcke [in *Aspects of Electron-Molecule Scattering and Photoionization*, edited by A. Herzenberg (AIP, New Haven, 1989), p. 169]. The dissociative-attachment cross sections are in reasonable agreement with experiment and with other theories.

I. INTRODUCTION

Inelastic processes in low-energy collisions of electrons with HCl molecules have been intensively studied since 1976 when Rohr and Linder¹ discovered a strong threshold peak in the vibrational-excitation (VE) cross section. The recent data of Knoth *et al.*² give new results for the angular distribution and the absolute magnitude of the cross section. Data for dissociative-attachment (DA) cross sections obtained by Allan and Wong³ were a new challenge for theory.

Since the late 1970s great progress has been made in the development of theory. Most of the theoretical models can be divided into two classes. The models of the first class (so-called resonance models) start with the resonance potential curve for HCl^- . Interaction with the electron continuum leads to the appearance of a nonlocal-complex potential (NCP) for the nuclear motion.⁴

The first calculation of the DA to the HCl molecule was done by Bardsley and Wadehra⁵ using a partly nonlocal approximation when the real part of the nonlocal potential was treated in the local approximation. Domcke and Mundel⁶ carried out calculations for VE and DA by the exact solution of the equations of nonlocal theory.

The theoretical models of the second class do not assume any resonance state of the ion. The threshold structure is explained in terms of virtual state⁷ and nuclear excited Feshbach resonances whose tails appear just above VE thresholds, as was suggested by Gauyacq and Herzenberg.⁸ Actually, models of the first class implicitly include features associated with virtual-state and Feshbach resonances since the adiabatic bound state of the negative ion becomes a virtual state at internuclear distances to

the left of the crossing point of the HCl and HCl^- curves, the so-called stabilization or merging point. However, the virtual state is not the major point of the resonance models.

The most striking feature of the nonresonant models is that in trying to reproduce the experimental data, the authors obtain the stabilization point lying very close to the equilibrium distance. If we let ρ be the internuclear distance relative to equilibrium, then the stabilization point ρ_{cr} varies between 0.15 and 0.20 a.u. in the effective range calculations of Teillet-Billy and Gauyacq,⁹ and actually equals 0.15 (as shown by Fabrikant¹⁰) in the calculations of Dube and Herzenberg.⁷ Apparently, putting $\rho_{\text{cr}}=0$ we would obtain a bound state with zero energy at the equilibrium distance. It means that the scattering phase shift in the fixed-nuclei approximation experiences a jump by $\pi/2$ at zero energy and the vibrational-excitation cross section reaches the unitarity limit at the threshold.¹⁰ In a more general case, when ρ is close to 0, the cross section rises very sharply at the threshold and falls off much more slowly in disagreement with the shape observed by Rohr and Linder¹ and Knoth *et al.*² *Ab initio* calculations¹¹⁻¹⁵ using standard structure methods yield $\rho_{\text{cr}} \approx 0.6$ a.u. As mentioned by Teillet-Billy and Gauyacq,⁹ all attempts to reproduce the experimental data with this merging point were unsuccessful.

Recently Morgan *et al.*¹⁶ carried out the first *ab initio* calculations of inelastic processes in e -HCl collisions using the R -matrix theory of Schneider *et al.*¹⁷ They also calculated the adiabatic potential curve for HCl^- and their value of ρ_{cr} is significantly lower than that obtained from the calculations using structure methods. They obtained $\rho_{\text{cr}}=0.24$ or 0.34 depending on the polarization model they chose. Naturally, in the first case they ob-

tained a sharper threshold peak. In order to include more completely the short-range interaction of the electron with the molecule, a rather large R -matrix radius in the electron coordinate ($r_0 = 10$ a.u.) was chosen. This led to five R -matrix poles necessary to describe the electron-molecule interaction in the fixed-nuclei approximation, and did not allow for a direct connection between the R -matrix theory and resonance theories.

The first R -matrix calculations¹⁸ of VE and DA in e -HCl collisions were not *ab initio* but semiphenomenological. In order to reduce the number of input parameters to the minimum, this theory started from the resonance expression for the R matrix in the fixed-nuclei approximation

$$R(\rho) = \frac{\gamma^2(\rho)}{E_1(\rho) - E_e} + R_r. \quad (1)$$

Here E_e is the electron energy, and $\gamma(\rho)$ and $E_1(\rho)$ are usual parameters of the R -matrix theory. R_r is a background term weakly dependent on ρ and E_e . For simplicity we will assume that R_r does not depend on ρ and E_e at all. The R matrix in the form (1) was used as input data for the theory including nonadiabatic effects, as was suggested by Schneider *et al.*¹⁷

Recently Fabrikant¹⁹ showed that such formulation of the R -matrix theory is completely equivalent to the nonlocal-complex-potential (NCP) theory. The major difference between the two theories is in the methods of evaluation of the input parameters. The only input data of the R -matrix theory are functions $\gamma(\rho)$ and $E_1(\rho)$ which can be calculated *ab initio*. All energy-dependent terms of the theory are calculated from the logarithmic derivatives of the electronic wave functions in different vibrational channels on the R -matrix sphere. These derivatives also incorporate long-range interaction between the electron and the molecule. In applications of the NCP theory it is necessary to postulate not only internuclear dependence but also energy dependence of the parameters.

The major deficiency of the results obtained by Fabrikant¹⁸ is that the VE cross sections near the threshold are very sensitive to the R -matrix radius in the internuclear coordinate. This problem could be solved self-consistently only in *ab initio* calculations of the type completed by Morgan *et al.*¹⁶ However, the difficulty can be eliminated even in the model approach if we would employ the equivalence between the R -matrix and NCP theories and calculate the DA cross sections using the NCP approach.

The purpose of the present paper is to obtain self-consistent results in the framework of the resonance R -matrix theory. Particularly, we study the following points which are important for both *ab initio* and model approaches.

(i) We investigate the dependence of the results on the number of vibrational levels of the neutral molecule included in calculations, since both nonlocal and R -matrix approaches show that even the vibrational continuum may be important for the problem.

(ii) We study the dependence of the results on the behavior of the ion potential curve near the stabilization

point. We investigate how this behavior is related to the results of *ab initio* calculations of the adiabatic potential curve.

(iii) We study oscillations in the VE cross sections near the threshold, the so-called boomerang phenomenon,²⁰ first theoretically predicted for the HCl molecule by Domcke.²¹

(iv) We discuss the shape of the threshold peak obtained from different theories.

An important part of the calculations includes an evaluation of the matrix elements of the Green's function for the nuclear motion in some effective potential. The direct computation of these matrix elements requires high-precision arithmetic. Kazansky and Yelets²² developed a quasiclassical method for evaluating this type of matrix elements. Recently, Kazansky and Kalin²³ used it to develop a quasiclassical NCP theory. Here we will use this approach to calculate the matrix elements of our theory with some modifications which will be discussed below. Therefore, our theory may be called the quasiclassical R -matrix theory.

II. BASIC THEORY

The basic theory has been discussed by Fabrikant^{18,19} and only the essential outlines will be given here. We will also discuss in more detail the method of evaluation of the DA cross sections based on the NCP theory.

We start from Eq. (1) for the R matrix in the fixed-nuclei approximation. To include vibrational dynamics as suggested by Schneider *et al.*,¹⁷ we introduce the operator

$$R(\rho) = \gamma(\rho)[H_I(\rho) - E]^{-1}\gamma(\rho) + R_r, \quad (2)$$

where

$$H_I(\rho) = T + U(\rho), \quad (3)$$

$$U(\rho) = V_0(\rho) + E_1(\rho), \quad (4)$$

where T is the kinetic-energy operator for the nuclear motion, $V_0(\rho)$ is the potential-energy function of the target molecule, and E is the total energy.

In order to calculate the VE cross section, let us consider the set of radial electron wave functions at $r > r_0$, which can be represented in the following matrix form:

$$u = u^- - u^+ S, \quad (5)$$

where S is the scattering matrix and u^\pm are diagonal matrices with the asymptotic form

$$u_v^\pm \sim k_v^{-1/2} e^{ik_v r}, \quad (6)$$

where e_v , $v = 0, 1, \dots$ are eigenenergies of the Hamiltonian for the neutral molecule and $k_v^2 = 2(E - e_v)$.

The S matrix describing the vibrational transitions can be calculated from the matching conditions

$$(u^- - u^+ S)|_{r=r_0} = R \frac{d}{dr} (u^- - u^+ S)|_{r=r_0}. \quad (7)$$

Redefining the channel functions as

$$\bar{u}^\pm = u^\pm - R_r \frac{d}{dr} u^\pm|_{r=r_0}, \quad (8)$$

we obtain the following expression for S :

$$S = \frac{\bar{u}^-}{\bar{u}^+} - \frac{2i}{\bar{u}^+} \gamma(E - T - V_{\text{opt}})^{-1} \gamma \frac{1}{\bar{u}^+}, \quad (9)$$

where

$$V_{\text{opt}} = U - \gamma L \gamma \quad (10)$$

and L is an operator function of $E - T - V_0$ with eigenvalues

$$L_{E_v} = \frac{1}{\bar{u}_{E_v}^+} \left. \frac{du_{E_v}^+}{dr} \right|_{r=r_0}, \quad (11)$$

where $E_v = k_v^2/2$. Equations (9) and (10) allow us to establish the direct connection between the resonance R -matrix theory and the NCP theory.¹⁹ We can use this relation to calculate the DA cross section without introducing the R -matrix radius in the internuclear coordinate. The cross section for the DA to the v th vibrational state in the NCP theory is defined as⁶

$$\sigma_{\text{DA},v} = \frac{4\pi^3}{k_v^2} |\langle v | V_{E_v} | \psi_E^{(+)} \rangle|^2, \quad (12)$$

where V_E is the coupling amplitude describing the interaction between the diabatic state and the continuum in the NCP theory and $\psi_E^{(+)}$ is the solution of the equation

$$(T + V_{\text{opt}} - E) \psi_E^{(+)} = 0, \quad (13)$$

with the outgoing-wave boundary condition. Using the relation¹⁹

$$V_E(\rho) = \frac{\gamma(\rho)}{\pi^{1/2} \bar{u}_E^+} \quad (14)$$

and defining the DA amplitude

$$y_v(E) = \langle v | \gamma | \psi_E^{(+)} \rangle, \quad (15)$$

we obtain

$$\sigma_{\text{DA},v} = \frac{4\pi^2}{k_v^2} \left| \frac{y_v(E)}{\bar{u}_{E_v}^+} \right|^2. \quad (16)$$

Using the representation of the eigenstates of the neutral Hamiltonian $T + V_0$, we have

$$V_{\text{opt}} = U - \sum \gamma |v\rangle L_{E_v} \langle v | \gamma, \quad (17)$$

where the symbol \sum means the summation over discrete states and integration over the continuum. Then the solution of Eq. (13) can be written in the form

$$\psi_E^{(+)} = \chi_E^{(+)} + \sum L_v y_v \int G^{(+)}(\rho, \rho') \gamma(\rho') \phi_v(\rho') d\rho', \quad (18)$$

where $\phi_v(\rho) = \langle \rho | v \rangle$ and

$$G_E^{(+)} = (H_I - E - i0)^{-1} \quad (19)$$

is the Green's function for the nuclear motion in the potential U and $\chi_E^{(+)}$ is the regular solution of the equation

$$(H_I - E) \chi_E = 0, \quad (20)$$

with the asymptotic form of the incident plus the outgoing wave.

Defining now the zero-order amplitude

$$\gamma_v(E) = \langle v | \gamma | \chi_E^{(+)} \rangle, \quad (21)$$

we obtain a set of linear equations for the amplitudes

$$y_v = \gamma_v + \sum_{v'} L_{v'} \langle v | \gamma G^{(+)} \gamma | v' \rangle y_{v'}. \quad (22)$$

Equation (22) is a set of algebraic equations if we include only discrete states in the right-hand side (r.h.s.), and it is a set of integro-matrix equations if we also include the continuum. After these equations are solved, the DA cross sections can be calculated directly from expression (16). The matrix elements $\langle v | \gamma G^{(+)} \gamma | v' \rangle$ can be also used for the calculation of the VE cross sections since, as follows from Eq. (7), the expression for the nondiagonal part of S can be written in the form

$$S^{nd} = -2i(\bar{u}^+)^{-1} (\gamma G^{(0)} \gamma L - 1)^{-1} \left[\frac{du^+}{dr} \right]^{-1}, \quad (23)$$

where $G^{(0)} = \text{Re} G^{(+)}$.

III. QUASICLASSICAL APPROACH

Evaluation of the matrix elements $\langle v | \gamma | \chi_E^{(+)} \rangle$ and $\langle v | \gamma G^{(+)} \gamma | v' \rangle$ requires high-precision arithmetic because of rapid oscillations in the integrands, especially when one deals with highly excited states. In order to facilitate the computations and get more physical insight into the problem, Kazansky and Yelets²² suggested the quasiclassical method for the Herzberg theory based on the stationary-point technique. When dealing with γ_v defined by Eq. (21), the method is straightforward and was discussed in detail elsewhere.^{22,18} The stationary point is defined by the generalized Franck-Condon condition

$$e_v - V_0(\rho_s) = E - U(\rho_s). \quad (24)$$

The evaluation of the matrix elements of $\gamma G^{(+)} \gamma$ is a more complicated problem. Using the spectral representation of the Green's function, we obtain

$$\langle v | \gamma G^{(+)} \gamma | v' \rangle = \sum \frac{\gamma_v(\epsilon) \gamma_{v'}(\epsilon)}{\epsilon - E - i0} d\epsilon, \quad (25)$$

where we have to sum over the discrete levels, if any, for the potential U .

Using the quasiclassical analytical expression for $\gamma_v(\epsilon)$, we can calculate this integral numerically. Since the stationary point ρ_s is a function of ϵ , we have a whole region of ρ contributing to the integral.

Another approach was suggested by Kazansky and Kalin.²³ Starting from the expression for the Green's function in coordinate space and applying the stationary-point method twice, they obtained analytical expression of the form

$$\langle v | \gamma G^{(+)} \gamma | v' \rangle = \pi \gamma_{v <} (E) \eta_{v >}^{\pm} (E), \quad (26)$$

where $v < = \min(v, v')$, $v > = \max(v, v')$, and

$$\eta_v^{(\pm)}(E) = \pm \langle v | \gamma | \xi_E^{(\pm)} \rangle, \quad (27)$$

where $\xi^{(\pm)}$ is the solution of Eq. (20) with the asymptotic form of outgoing (for positive sign) or ingoing (for negative sign) wave, and we have the positive sign if $\rho_s > 0$ and the negative sign if $\rho_s < 0$.

The results of calculations of the matrix elements show that the two approaches are roughly in agreement within the accuracy of the quasiclassical approximation. However, since Eq. (26) was obtained by the double use of the stationary-point method and represents the contribution due to only one stationary point $\rho_s(E)$, we consider Eq. (25) as more accurate. Also, Eq. (26) cannot be used below the DA threshold.

IV. THE ROLE OF THE VIBRATIONAL CONTINUUM AND LONG-RANGE BEHAVIOR OF THE OPTICAL POTENTIAL

The crucial question for application of the method described above is how many vibrational states we have to include in Eq. (22) or in the similar equation for the VE S matrix. Domcke and Mundel^{6,24} and Fabrikant^{18,19} pointed out that even the vibrational continuum is important for the calculation of the cross sections. In order to understand this point, we can consider the dependence of $\gamma_v(\epsilon)$ on v . The function $\gamma_v(\epsilon)$ is non-negligible if the root ρ_s of Eq. (24) is real and lies in the classically allowed region. In Fig. 1 we demonstrate the dependences of ρ_s and the right turning point for V_0 on e_v for the energy ϵ near the DA threshold. The stationary point is real for

$$e_v < e_{\max} = E_D + \epsilon - U(\infty),$$

where E_D is the dissociation limit. We see from Fig. 1 that e_{\max} lies in the vibrational continuum. This is a consequence of the mainly repulsive character of the potential curve $U(\rho)$. If $U(\rho)$ would have a large attractive part, as in the case of N_2 , the main contribution to the

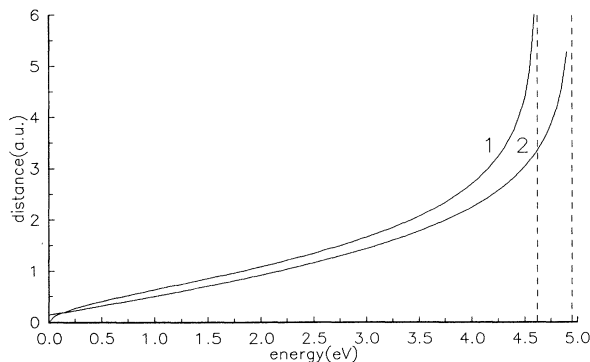


FIG. 1. The dependence of the stationary point ρ_s (curve 1) and the right turning point for the curve $V_0(\rho)$ (curve 2) on the energy e of the neutral molecule for the total energy $E = 1$ eV. Parameters of the potential curve $U(\rho)$ correspond to model 1 (see Table I). The dashed vertical lines denote asymptotes.

process would be given by $\epsilon < U(\infty)$ and the vibrational continuum would be inessential.

In making this conclusion, we assumed that $\gamma(\infty) \neq 0$. This is usually the case in the R -matrix theory, and, as a consequence, $U(\infty)$ in the R -matrix theory does not correspond exactly to the DA threshold, or, in other words, $E_D - U(\infty)$ is not exactly equal to the electron affinity A of Cl.

Since the solution of Eq. (13) for the nuclear motion should have the correct asymptotic behavior, we should assume that the nonlocal part of the optical potential should have a long-range part nonvanishing at infinity. Indeed, at large ρ we have

$$V_{\text{opt}} \sim U(\infty) - \gamma^2(\infty) \sum_v |v\rangle L_{E_v} \langle v|, \quad (28)$$

and both local and nonlocal parts are nonzero.

Equation (28) shows that the part of the nonlocal potential, nonvanishing at infinity, simply compensates the part of U which differs from $E_D - A$ at infinity, and we should not have any unphysical effects at $\rho \rightarrow \infty$. However, from the computational point of view the long-range behavior of the nonlocal part may cause some difficulties.

In order to facilitate our treatment, we will use the local approximation for the long-range part. At a very large ρ only highly excited states and the vibrational continuum make an essential contribution to the nonlocal part of the optical potential (17). If the energy E lies well below the dissociation limit, we can neglect the dependence of L_{E_v} on E_v for these states and get

$$V_{\text{opt}} - U(\infty) \approx -\gamma^2(\infty) L_{\bar{E}_v} \delta(\rho - \rho'), \quad (29)$$

where $\bar{E}_v = E - \bar{e}_v$ and \bar{e}_v is some mean excitation energy lying above the dissociation limit. We can obtain the actual value of $L_{\bar{E}_v}$ from the condition $U(\infty) - \gamma^2(\infty) L_{\bar{E}_v} = E_{\text{DA}}$, where E_{DA} is the DA threshold.

For concrete calculations it is convenient to write down the function $\gamma(\rho)$ in the form

$$\gamma(\rho) = \gamma_s(\rho) + \gamma_l(\rho), \quad (30)$$

where $\gamma_s(\rho) \rightarrow 0$ for $\rho \rightarrow \infty$ and $\gamma_l(\rho) \rightarrow \gamma(\rho)$ for $\rho \rightarrow \infty$.

Now, using the local approximation for the long-range part, we have

$$V_{\text{opt}} = U - \sum_v \gamma_s |v\rangle L_{E_v} \langle v| \gamma_s + \Delta U, \quad (31)$$

where

$$\Delta U(\rho) = -L_{\bar{E}_v} \gamma_l(\rho) [2\gamma_s(\rho) + \gamma_l(\rho)]. \quad (32)$$

A simple parametrization for $\gamma_l(\rho)$ may be chosen in the following form:

$$\gamma_l(\rho) = \begin{cases} 0, & \rho < \rho_0 \\ \gamma(\rho)(1 - e^{-(\rho - \rho_0)^\eta})^2, & \rho > \rho_0 \end{cases} \quad (33)$$

and

$$\gamma_s(\rho) = \gamma(\rho) - \gamma_l(\rho). \quad (34)$$

A parametrization of this type was used in nonlocal theories^{5,6} for the width function directly connected with the coupling amplitude (14) in order to avoid the long-range behavior of the optical potential. Here we have chosen a form which gives sufficiently smooth behavior of $\Delta U(\rho)$.

The parameter ρ_0 is the distance beyond which the nonlocal potential can be treated in the local approximation. This distance should correspond to the right turning point of the vibrational state starting from which we can neglect the energy dependence of the logarithmic derivative L_{E_v} . For the calculations in the region not far from the DA threshold, we can choose $\rho_0 > 1$. This corresponds to the right turning point of the level $v = 5$.

In some sense we are returning to the R -matrix radius in the internuclear coordinate. However, in contrast with the previous work,¹⁸ the choice of this radius is now physically grounded, and calculations do not indicate any dependence on ρ_0 when ρ_0 increases from 1 a.u. to larger values.

The modification of the nonlocal potential considered above leads to an upper limit of ρ_s values contributing to the matrix elements $\gamma_v(\varepsilon)$ and $(\gamma G \gamma)_{vv'}$. As we see from Fig. 1, choosing the limit in the region of 1 a.u. allows us to neglect the vibrational continuum. It should be emphasized that this becomes possible only after modification of the optical potential, and reflects specific features of the e -HCl scattering. For example, if the DA threshold were lower, the inclusion of the vibrational continuum would be necessary even after the modification of the optical potential.

V. DIABATIC AND ADIABATIC POTENTIAL CURVES

The optical potential can now be represented in the form

$$V_{\text{opt}} = U_d(\rho) - \sum_v \gamma_s |v\rangle \langle v| \gamma_s, \quad (35)$$

where

$$U_d(\rho) = U(\rho) + \Delta U(\rho) \quad (36)$$

is equivalent to the diabatic potential curve of the NCP theory. However, they are not completely identical because of some arbitrariness in their definitions in both theories. In the NCP theory this arbitrariness follows from the definition of the P and Q space in the Fano-Bardsley approach, and in the R -matrix theory from the way of inclusion of the long-range part of the nonlocal potential. In order to get a direct connection with *ab initio* calculations for the HCl^- system, it is better to consider the adiabatic potential curve at $\rho > \rho_{\text{cr}}$. This curve may be obtained by solving the equation

$$R(\rho) = \frac{u(r_0)}{u'(r_0)} \quad (37)$$

for the electron energy $E_e(\rho)$, where u and u' are the radial function and its derivative in the fixed-nuclei approx-

TABLE I. Parameters (in a.u.) of the potential curve.

Model	$U(\rho) = Be^{-2\beta\rho} - Ce^{-\beta\rho} + D$			
	β	B	C	D
1	2.026	0.041 56	0.011 05	0.024 62
2	1.690	0.023 90	0	0.025 0
3	2.026	0.061 56	0.031 05	0.024 62

imation. The adiabatic potential energy can then be obtained as

$$U_{\text{ad}}(\rho) = V_0(\rho) + E_e(\rho). \quad (38)$$

In our first calculations^{10,18} of e -HCl scattering we chose $U(\rho)$ by fitting $U_{\text{ad}}(\rho)$ to the results of the stabilization calculations of Goldstein *et al.*¹¹ Since that time, a number of new calculations of $U_{\text{ad}}(\rho)$ have been done.¹²⁻¹⁶ The multiconfiguration self-consistent-field (MCSCF) calculations of O'Neil *et al.*¹⁴ seem to be most precise.

In order to compare our results with these data, we started from the Morse potential curve for $U(\rho)$. The calculations have been done using three sets of the Morse parameters listed in Table I. Set 1 corresponds to the adiabatic potential curve which gives the best fit to *ab initio* results of O'Neil *et al.*¹⁴ At the same time we tried to preserve the same form of the curve near $\rho = 0$ as in the old version^{10,18} in order to fit the eigenphase sum to that obtained from *ab initio* calculations of Padiál *et al.*²⁵ As we see from Fig. 2, the resulting $U_{\text{ad}}(\rho)$ fits the data of O'Neil *et al.* quite well, but of course the Morse function for $U(\rho)$ is not flexible enough to reproduce all details of the *ab initio* curve. It should also be mentioned that the Morse potential curve does not give the proper asymptotic behavior

$$U(\rho) = -\frac{\alpha}{2(\rho + R_e)^4}, \quad (39)$$

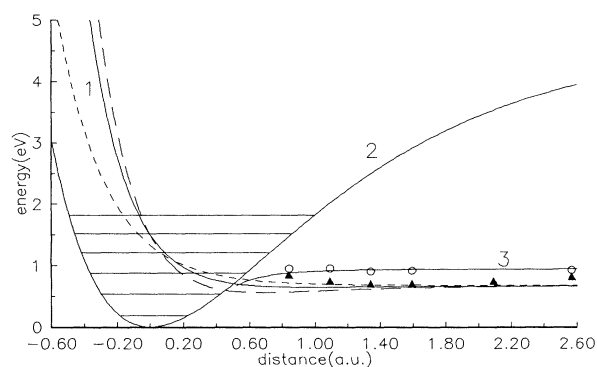


FIG. 2. Potential curves of the problem. Solid curves: 1, $U(\rho)$, for model 1; 2, potential curve $V_0(\rho)$ for the neutral molecule; 3, adiabatic potential curve corresponding to curve 1. Circles, *ab initio* calculations of O'Neil *et al.* (Ref. 14) of adiabatic energies. Triangles, *ab initio* calculations of Krauss and Stevens (Ref. 12). Short-dashed curve, $U(\rho)$ for model 2. Long-dashed curve, $U(\rho)$ for model 3. Horizontal lines indicate vibrational levels of the neutral molecule.

where $\alpha=4.5$ a.u. is the polarizability of the H atom. However, as was found by O'Neil *et al.*, the *ab initio* curve starts to fit the expression (39) only at a rather large distance of $\rho \approx 2.6$. The contribution of distances $\rho > 2.6$ is not important in our calculations with $\rho_0 \approx 1$.

On the other hand, we see a rather strong disagreement between the results of two *ab initio* calculations. The curve of Krauss and Stevens¹² has a well-pronounced minimum at $\rho \approx 1.6$ a.u. and is very close in energy to the asymptote at the crossing, whereas the curve of O'Neil *et al.* shows a more shallow minimum and turns attractive again at distances near ρ_{cr} . This behavior was confirmed by the calculations of Raizmann *et al.*,¹⁵ who found that the curve falls down towards the unbound region from the inflection at $\rho \approx 1.65$ a.u. The same features are exhibited in the curve obtained by Morgan *et al.*¹⁶

The overall behavior of the $U(\rho)$ curve used in this paper is quite similar to that used in the old version of the theory, but it differs somewhat near the crossing point ρ_{cr} which is very important for the VE cross sections, as we will see later. The function $\gamma(\rho)$ affects mainly the behavior of the eigenphase sum and it remained in the same form as in the old version.

VI. RESULTS AND DISCUSSION

When performing the calculations of the VE and DA cross sections, we first investigated the dependence of the results on ρ_0 . This dependence turned out to be very weak for $\rho_0 \geq 1$ a.u. which confirms our assumption about the validity of the local approximation for $\rho \geq 1$ a.u. The dependence of the VE cross sections on the number of vibrational levels is more essential and is demonstrated in Figs. 3, 4, and 5. For the value of the parameter ρ_0 of about 1 a.u., the transition points ρ_s up to 2 a.u. may be essential, which roughly corresponds to $v=15$ for a typical energy $\epsilon=1$ eV. Therefore, we can expect convergence starting from this value of v . Indeed, the results for $v_{max}=14$ and 20 differ slightly for VE of the $v=1$ level. For VE of the $v=2$ and 3 levels the convergence is poor-

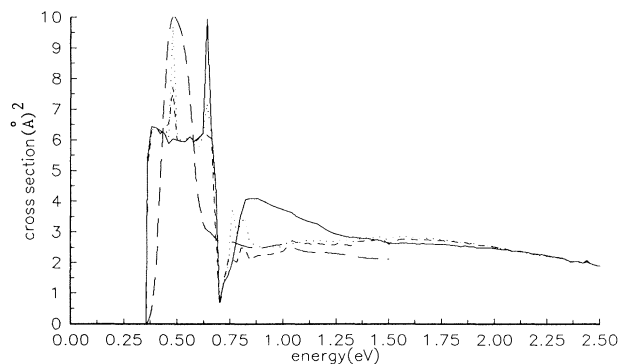


FIG. 3. Vibrational excitation of HCl ($v=1$), results of model 1. Solid curve, $v_{max}=8$; dashed curve, $v_{max}=14$; dotted curve, $v_{max}=20$. Long-dashed curve, experimental results of Knoth *et al.* (Ref. 2).

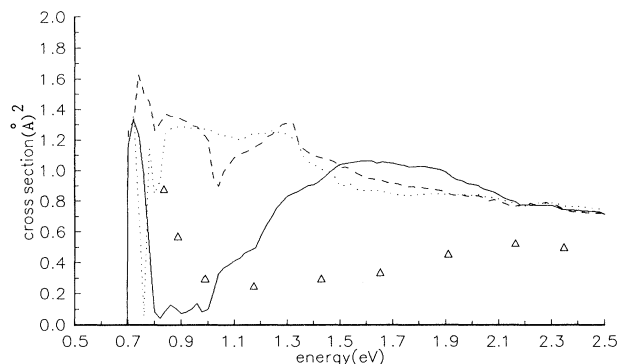


FIG. 4. The same as in Fig. 3 for $v=2$. Triangles are experimental data of Rohr and Linder (Ref. 1).

er, and we still see an essential difference between the cases $v_{max}=14$ and 20. However, for $v_{max}=24$ (the edge of the discrete spectrum), the results are almost indistinguishable from that of $v_{max}=20$.

The convergence of the cross sections with v_{max} is better for higher energies. When the electron energy increases and becomes large compared to the vibrational spacing, nonadiabatic effects become inessential. As a result, only small ρ , corresponding to the classically allowed region for the initial and final vibrational states, contribute to the process. Virtual transitions to higher vibrational states, which occur at larger ρ , become inessential.

For $v_{max}=8$ the threshold peak appears in all cross sections presented in Figs. 3–5. However, the increase of v_{max} leads to the suppression of the peak in the cases $v=2$ and 3. In the first case we still have the threshold peak but the following rise of the cross section leads to essential disagreement with the experimental results of Rohr and Linder.¹ Also, the absolute magnitude of the cross section for $v=2$ is too large compared to the experiment and other theories. In the case $v=3$ the suppression of the threshold peak agrees with the results of Domcke and Mundel⁶ but the absolute magnitude of the cross section is too large compared with their maximum

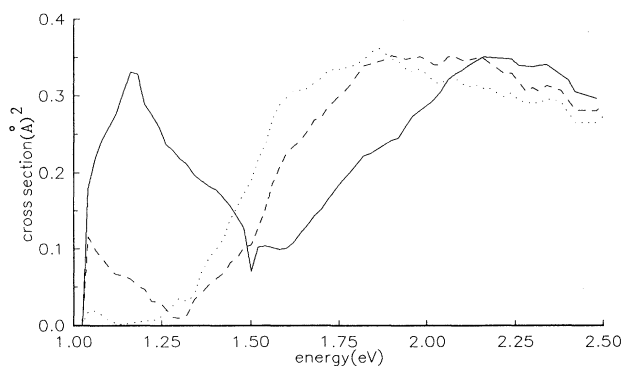


FIG. 5. The same as in Fig. 3 for $v=3$.

value of about 0.1 \AA^2 . In this case we have better agreement in absolute magnitude with Morgan *et al.*¹⁶ They obtained the maximum value of about 0.37 \AA^2 but their maximum occurs near the threshold whereas our cross section has the maximum at $E \approx 2.2 \text{ eV}$.

Let us turn now to the discussion of the $v=1$ cross section. As in most calculations, we see a sudden drop of the $v=1$ cross section at the $v=2$ threshold, followed by a sharp rise. What is new in our results is that we obtained small-scale oscillations in the region of the threshold peak. These oscillations were first discussed by Domcke²¹ as a boomerang phenomenon²⁰ namely, the interference of the outgoing wave in HCl^- with a weak incoming component which has been reflected by the attractive part of the HCl^- potential curve at large ρ . Domcke obtained these oscillations right above the threshold peak. In our calculations they are seen also in the threshold-peak region. A slight variation of the potential curve for HCl^- in the region near ρ_{cr} can drastically affect the form and absolute value of the threshold peak. This is demonstrated in Figs. 6 and 7 where we present the results for VE using our old potential curve,¹⁸ and a curve which is more attractive in the region near ρ_{cr} . Note that in the last case we have a rather large absolute value of the VE cross section at the threshold peak which exceeds the experimental result. In contrast with non-resonant theories we obtain such a large value when ρ_{cr} is still quite far from $\rho=0$ (namely, $\rho_{\text{cr}}=0.45$). Since the VE cross sections, especially for $v=2$, are too large in this model, we consider it less realistic.

In his time-dependent treatment of the problem, Domcke introduced two time scales corresponding to the time decay of the $^2\Sigma$ shape resonance (which traps the electron to form the HCl^- state) and the time of the oscillatory nonexponential decay of HCl^- which is responsible for the threshold peak. As we can see from the boomerang phenomenon, one can introduce a third time scale corresponding to the time of motion of the nuclei in some effective potential until the reflection. However, it is difficult to relate this potential to any of the fixed-nuclei potentials (diabatic or adiabatic). Although discrete states in these potentials do exist due to the long-range polarization part, it is not the polarization that causes these oscillations because they are mainly affected by the behavior of the potential near the crossing point. We think that the nonlocality of the problem is the crucial point for the form of the threshold peak and the boomerang oscillations. However, a simple physical picture explaining this relationship still does not exist. The time-dependent approach of Domcke and Gertitschke^{21,26} seems to be quite promising in that regard.

The boomerang oscillations were not obtained in *ab initio* calculations.¹⁶ Apparently, this means that for the appearance of the oscillations the resonance approximation is important. If few resonance terms were included in the theory, the oscillations would probably be smoothed out.

Since nonadiabatic and nonlocal effects are very important near threshold, we cannot associate directly the threshold peak with an S -matrix pole. The existence of an isolated S -matrix pole near the threshold would lead

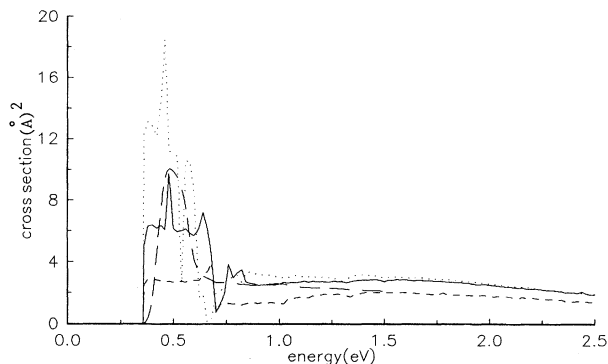


FIG. 6. Comparison of the results from different models for VE of $v=1$. Solid curve, model 1; dashed curve, model 2; dotted curve, model 3 (see Table I); long-dashed curve, experimental results of Knoth *et al.* (Ref. 2).

to either the Breit-Wigner form of the threshold peak or to the form typical for the virtual or bound state near the threshold,²⁷

$$\sigma \propto \frac{k}{\kappa^2 + k^2} \quad (40)$$

(κ being a parameter) with some modifications for polar molecules.²⁸ Neither of these forms was obtained in the resonance theory of Domcke and Mundel⁶ and in our approach. However, the investigation of the S -matrix poles would be useful for the further understanding of the problem and may be done using the explicit expression (9) for the S matrix.

At this point it is worthwhile to mention that in nonresonance theories⁷⁻⁹ the threshold peak is associated with a virtual state at $\rho < \rho_{\text{cr}}$ which gives another form of the threshold peak than that observed experimentally. Namely, the cross section has a very sharp rise with a more moderate falloff as described by Eq. (40). In contrast, a resonance theory gives a broad peak with superimposed structure. The *ab initio* calculations of Morgan *et al.*¹⁶ using polarized pseudostates look like the non-resonant model results, whereas their static-exchange-

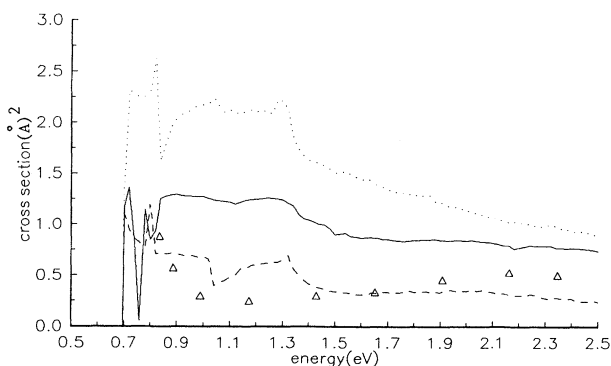


FIG. 7. The same as in Fig. 6 for $v=2$. Triangles are experimental data of Rohr and Linder. (Ref. 1).

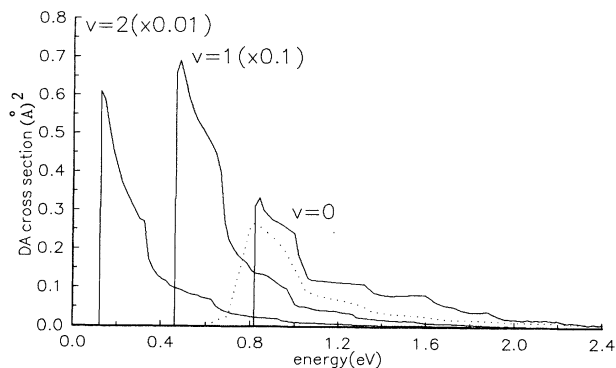


FIG. 8. DA cross section. Dotted curve, experimental data of Abouaf and Teillet-Billy (Ref. 29) for DA to $v=0$ normalized to the measurement of Orient and Srivastava (Ref. 30) at the peak.

polarization results look like the resonant model results of Domcke and Mundel,⁶ except for the superimposed structure obtained by Domcke and Mundel. The experimental results are between the two sets of results of Morgan *et al.*¹⁶

As in all resonance theories, we also obtained the broad $^2\Sigma$ shape resonance which was observed experimentally.¹ However, the position of this resonance is shifted to lower energies due to the rather small value (about 1.5 eV) of the vertical attachment energy in our calculations.

The discussion presented above confirms our point¹⁹ that the resonance theory is adequate for the description of all features of the VE cross section. However, the parameters of the model should be calculated with a very high accuracy in order to reproduce the experimental data near the threshold.

Another essential feature of *ab initio* calculations of $U(\rho)$ should be the proper account of the higher angular modes for the projectile electron, since all model theories (including the present one) take into account only the lowest angular mode, which is mainly an *s*-wave mode. Recent experimental results of Knoth *et al.*² show essentially a nonisotropic angular distribution of electrons in

the final state, indicating that the inclusion of the higher modes is necessary for a proper calculation of the threshold peak.

Let us now turn to the discussion of the results for the DA cross sections. They do not exhibit as strong a dependence on the number of vibrational levels as the VE cross section and change very slightly starting from $v_{\max}=8$. In Fig. 8 we present cross sections for DA to different vibrationally excited states of the HCl molecule and compare the data for $v=0$ with the experimental results of Abouaf and Teillet-Billy²⁹ normalized to the measurements of Orient and Srivastava.³⁰ We have also studied the isotope effect—namely, DA to the DCl molecule. The comparison of peak values between different theories and experiments is presented in Table II. Like all other theories, our theory gives values that are too low for DA to $v=2$, both for HCl and DCl as compared to the experimental values. Also, our cross section for DA to $v=0$ falls off too slowly in the energy region between 1 and 2 eV. Otherwise, the agreement with the experiment is good. The stepwise structure of the cross section at the VE thresholds discussed in experimental²⁹ and theoretical^{6,18} papers is very well pronounced.

VII. CONCLUSION

Although the first results¹⁶ of *ab initio* calculations of the inelastic processes in *e*-HCl collisions have already appeared, it seems that model calculations are still very useful for at least two reasons. That is, they allow us to get a better understanding of the physics of the processes and give directions for *ab initio* calculations. Accordingly, we can conclude the following from the present work.

A large number of vibrational states of the neutral molecule should be included in order to get a convergence in the close-coupling or *R*-matrix calculations. In order to exclude the vibrational continuum, the long-range part of the NCP should be added to the *R*-matrix potential curve $U(\rho)$ to obtain the physical DA threshold for $U(\infty)$. The corresponding modification of the function $\gamma(\rho)$ should also be completed. This procedure corresponds to the local approximation for the long-range part of the NCP.

TABLE II. Peak values (in \AA^2) of the cross sections for the DA to HCl and DCl in vibrational states $v=0, 1, 2$.

v	HCl					DCl			
	Theory		Expt.			Theory		Expt.	
0	0.33 ^a	0.14 ^b	0.30 ^c	0.2 ^d	0.52 ^e	0.266 ^f	0.042 ^a	0.033 ^c	0.054 ^f
1	6.90 ^a	1.30 ^b	5.1 ^c	6.0 ^d	9.0 ^e	10.1 ^f	0.68 ^a	0.66 ^c	1.73 ^f
2	61.0 ^a	100 ^b	44 ^c	80 ^d	24 ^e	234 ^f	8.33 ^a	6.0 ^c	31.3 ^f

^aPresent, model 1.

^bBardsley and Wadehra (Ref. 5).

^cDomcke and Mundel (Ref. 6).

^dTeillet-Billy and Gauyacq (Ref. 9).

^eMorgan *et al.* (Ref. 16).

^fExperimental data are taken from the paper of Domcke and Mundel (Ref. 6), who combined different absolute and relative measurements (Refs. 3, 30, and 31) to obtain these values.

The absolute value of the VE cross section at the threshold peak is determined primarily by the interaction between vibrational states of the neutral molecule and the eigenstates of H_I near the region $\rho \approx \rho_{cr}$. Very accurate *ab initio* calculations of $U(\rho)$ in the region near ρ_{cr} should be performed to get a realistic VE cross section at the threshold peak. On the other hand, the form of the threshold peak may be strongly affected by the boomerang oscillations first found for HCl by Domcke²¹ in the region right above the threshold peak.

The resonance approach or any other theory implicitly including the resonance concept (such as *ab initio* R-

matrix theory) seems to be adequate for the description of inelastic processes in e -HCl collisions. We believe that any other approach using a single potential curve for the description of the HCl^- ion, such as the frame transformation theory of Greene and Jungen³² can be applied for this problem.

ACKNOWLEDGMENTS

This work has been supported by the National Science Foundation through Grant No. PHY-9006612.

-
- ¹K. Rohr and F. Linder, *J. Phys. B* **9**, 2521 (1976).
²G. Knoth, M. Radle, M. Gote, H. Ehrhardt, and K. Jung, *J. Phys. B* **22**, 299 (1989).
³M. Allan and S. F. Wong, *J. Chem. Phys.* **74**, 1687 (1981).
⁴J. N. Bardsley, *J. Phys. B* **1**, 349 (1968).
⁵J. N. Bardsley and J. M. Wadehra, *J. Chem. Phys.* **78**, 7227 (1983).
⁶W. Domcke and C. Mundel, *J. Phys. B* **18**, 4491 (1985).
⁷L. Dube and A. Herzenberg, *Phys. Rev. Lett.* **38**, 820 (1977).
⁸J. P. Gauyacq and A. Herzenberg, *Phys. Rev. A* **25**, 2959 (1982).
⁹D. Teillet-Billy and J. P. Gauyacq, *J. Phys. B* **17**, 4041 (1984).
¹⁰I. I. Fabrikant, *J. Phys. B* **18**, 1873 (1985).
¹¹E. Goldstein, G. A. Segal, and R. W. Wetmore, *J. Chem. Phys.* **68**, 271 (1978).
¹²M. Krauss and W. J. Stevens, *J. Chem. Phys.* **74**, 570 (1981).
¹³M. Bettendorff, R. J. Buenker, and S. D. Peyerimhoff, *Mol. Phys.* **50**, 1363 (1983).
¹⁴S. V. O'Neil, P. Rosmus, and D. W. Norcross, *J. Chem. Phys.* **85**, 7232 (1986).
¹⁵M. Rajzmann, F. Spiegelmann, and J. P. Malrieu, *J. Chem. Phys.* **89**, 433 (1988).
¹⁶L. A. Morgan, P. G. Burke, and C. J. Gillan, *J. Phys. B* **23**, 99 (1990).
¹⁷B. I. Schneider, M. LeDourneuf, and P. G. Burke, *J. Phys. B* **12**, L365 (1979).
¹⁸I. I. Fabrikant, *Z. Phys. D* **3**, 401 (1986).
¹⁹I. I. Fabrikant, *Comments At. Mol. Phys.* **24**, 37 (1990).
²⁰A. Herzenberg, *J. Phys. B* **1**, 548 (1968).
²¹W. Domcke, in *Aspects of Electron-Molecule Scattering and Photoionization*, edited by A. Herzenberg (AIP, New Haven, 1989), p. 169.
²²A. K. Kazansky and I. S. Yelets, *J. Phys. B* **17**, 4767 (1984); I. S. Yelets and A. K. Kazansky, *Zh. Eksp. Teor. Fiz.* **82**, 450 (1982) [*Sov. Phys.—JETP* **55**, 258 (1982)].
²³A. K. Kazansky, in *Some Aspects of the Atomic Collision Theory*, edited by V. I. Ochkur (Leningrad State University, Leningrad, 1986) (in Russian), p. 95; S. A. Kalin and A. K. Kazansky, *J. Phys. B* **23**, 809 (1990).
²⁴C. Mundel and W. Domcke, *J. Phys. B* **17**, 3593 (1984).
²⁵N. T. Padial, D. W. Norcross, and L. A. Collins, *Phys. Rev. A* **27**, 141 (1983).
²⁶P. L. Gertitschke and W. Domcke, *Z. Phys. D* **16**, 189 (1990).
²⁷L. D. Landau and E. M. Lifshits, *Quantum Mechanics* (Pergamon, Oxford, 1965).
²⁸I. I. Fabrikant, *Zh. Eksp. Teor. Fiz.* **73**, 1317 (1977) [*Sov. Phys.—JETP* **46**, 693 (1977)]; *J. Phys. B* **11**, 3621 (1978).
²⁹R. Abouaf and D. Teillet-Billy, *J. Phys. B* **10**, 2261 (1977).
³⁰O. J. Orient and S. K. Srivastava, *Phys. Rev. A* **32**, 2678 (1985).
³¹R. Azria, L. Roussier, R. Paineau, and M. Tronc, *Rev. Phys. Appl.* **9**, 469 (1974).
³²C. H. Greene and Ch. Jungen, *Phys. Rev. Lett.* **55**, 1066 (1985).